Density-dependent dynamics of exciton magnetic polarons in ZnMnSe/ZnSSe type-II quantum wells

A. A. Toropov, Ya. V. Terent'ev, S. V. Sorokin, and S. V. Ivanov
Ioffe Physico-Technical Institute, Russian Academy of Sciences, St. Petersburg 194021, Russia

T. Koyama, K. Nishibayashi, A. Murayama, and Y. Oka
Institute of Multidisciplinary Research for Advanced Materials, Tohoku University, Sendai 980-8577, Japan

J. P. Bergman, I. A. Buyanova, W. M. Chen, and B. Monemar
Department of Physics, Chemistry and Biology, Linköping University, S-581 83 Linköping, Sweden
(Received 17 January 2006; revised manuscript received 10 April 2006; published 28 June 2006)

We report on time-resolved photoluminescence studies of exciton dynamics in a ZnMnSe/ZnSSe type-II quantum well. Strong separation of the electrons, confined to the nonmagnetic semiconductor ZnSSe, and holes, confined to the diluted magnetic semiconductor ZnMnSe, results in an exciton lifetime exceeding 3 ns. Two excitonic emission lines are observed in this structure at low temperatures. The lower-energy line was associated with the formation of an exciton magnetic polaron (EMP), whereas the higher-energy line was attributed to the emission of nonmagnetically localized excitons. The intensity of the EMP line was found to saturate at a relatively low density of photoexcited carriers well below the exciton Mott density. This behavior evidences a limited density of sites where the hole localization radius is small enough to ensure the fast formation of EMP's with a noticeable binding energy.

DOI: 10.1103/PhysRevB.73.245335 PACS number(s): 73.21.Fg, 75.50.Pp, 78.47.+p

I. INTRODUCTION

One of the most spectacular phenomena observed in diluted magnetic semiconductors (DMS) is the formation of an exciton magnetic polaron (EMP)—a small region where magnetization is enhanced due to the exchange coupling between the spins of the magnetic ions and the exciton spin.[1] EMP's were detected and studied in bulk DMS, like, e.g., CdMnSe[2] and CdMnTe,[3–6] and DMS quantum wells (QW's) (e.g., CdTe/CdMn(Mg)Te QW's[7–9] and ZnSe/ZnMnSe QW's[10,11]). The issue of EMP stability was addressed both theoretically and experimentally. It was calculated that magnetic autolocalization of a free exciton, which can be considered as the formation of a free EMP, is impossible in bulk DMS, but can be achieved in DMS QW's with strong carrier confinement.[12] Nevertheless, it is generally accepted at present that the EMP formation in real DMS structures at liquid He temperatures is always preceded by a primary exciton localization induced by some mechanism other than the exchange coupling.[8,12–14] For bulk DMS layers it can be the localization due to the alloy disorder or the Coulomb interaction with a donor or acceptor impurity. In a DMS QW the in-plane localization can additionally result from potential fluctuations induced by interface roughness. It was suggested that magnetic fluctuations can also contribute to the primary localization process.[6,11,12,14,15]

In spite of the long history of intensive studies, there are still some unclear issues concerning the dynamics of formation and recombination of EMP's. In particular, several groups have reported on the coexistence of various types of excitons in the same bulk DMS layer or DMS QW structure, resulting in the simultaneous observation of different excitonic emission lines.[3,6,9,10] Two photoluminescence (PL) lines observed in bulk CdMnTe crystals were interpreted as emission of the EMP localized primarily by the fluctuations of magnetization and the emission of EMP bound to a neutral impurity, either acceptor[3] or donor.[6] In CdMgTe-CdTe-CdMnTe asymmetric QW's, the two lines were attributed to the recombination of excitons confined in the quantum-well region (higher-energy line) and the emission of excitons trapped at alloy fluctuations located at the magnetic interface (lower-energy line).[9] The formation of the EMP was associated only with the lower-energy excitonic line. The simultaneous observation of these two lines was also discussed in terms of the effect of the "EMP bifurcation."[9,16] In the ZnSe/ZnMnSe QW's the higher-energy PL line was explained as the recombination of free excitons confined in the ZnSe QW, whereas the lower-energy peak was identified as a type-II EMP with the electron confined to the nonmagnetic ZnSe layer and the hole trapped within the magnetic ZnMnSe layer.[10] In these studies the interplay of different localization processes could hardly be revealed due to the fast radiative recombination of the involved type-I excitons. Specifically, the localization dynamics of the quantum-well excitons, determined by the trapping of the hole near or within the magnetic barrier layer remains to be understood.

Another controversial issue concerns the density-dependent behavior of excitons in DMS structures. Several theoretical works have recently predicted the possibility of ferromagnetic ordering of the spins of magnetic ions under high excitation density. The existence of an attractive force between EMP's with parallel magnetic momenta was theoretically demonstrated, which, in principle, allows the formation of the magnetic bipolarons,[17] or even the coalescence of the EMP's within a ferromagnetic cluster.[18] The latter theory was used to interpret the recently reported observation of a giant mobility of EMP's in ZnSe/ZnMnSe QW's[19] as a manifestation of the exchange induced Bose condensation of

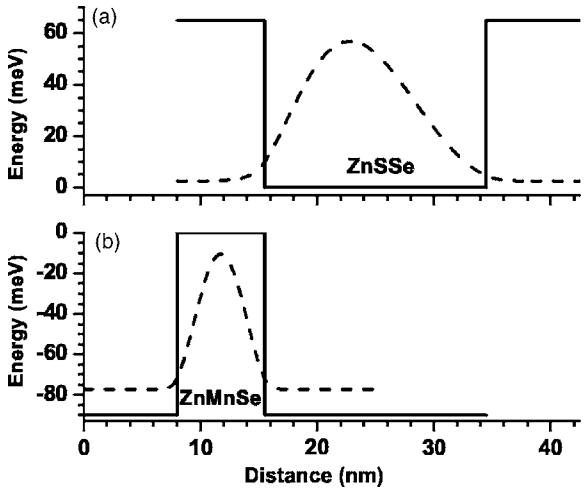

FIG. 1. Conduction (a) and valence (b) band lineups in the ZnMnSe/ZnSSe type-II QW. Dashed curves represent the calculated probability distribution of the electron and heavy hole along the quantization axis within the ground-state exciton at a zero magnetic field.

EMP's. On the other hand, recent studies of time-resolved PL of high-density EMP's in CdMnTe have demonstrated that the EMP at high-density conditions is unstable.[20]

In this paper we report on the investigation of the exciton dynamics in type-II QW's ZnSSe/ZnMnSe. The electrons in these structures are confined to the nonmagnetic ZnSSe layers and the heavy holes are confined to the magnetic ZnMnSe layers as a result of the intrinsic band offsets at the ZnSSe/ZnMnSe interface (see Fig. 1).[21] The PL spectra of such structures demonstrate two excitonic lines, the lower-energy line being associated with the EMP formation process.[22] This reminds us of the behavior reported for ZnSe/ZnMnSe QW's in Ref. 10. In contrast to the ZnSe/ZnMnSe QW's, the recombination time for all excitonic states in the ZnSSe/ZnMnSe QW's can be relatively long (in the range of a few nanoseconds) due the spatial separation of the electron and hole wave functions. Therefore the localization processes are not interrupted by exciton recombination and can be studied until establishing quasiequilibrium conditions. Furthermore, the long exciton lifetime allows one to study the density-dependent effects, even at moderate levels of excitation. It has been found that the increase in the excitation power density results in fast saturation of the EMP line in favor of the higher-energy line attributed to the emission of nonmagnetically localized excitons. This evidences a rather limited density of sites within the ZnMnSe layer, allowing the efficient magnetic localization of the holes.

The paper is organized as follows. In Sec. II we describe the design, fabrication, and x-ray diffraction studies of the samples containing ZnSSe/ZnMnSe multiple QW's. In Sec. III we present the results of time-resolved PL spectroscopy for different magnetic fields, average excitation power densities, and temperatures. In Sec. IV we analyze qualitatively the peculiarities of exciton localization processes in ZnSSe/ZnMnSe QW's, which can be responsible for the observed easy saturation of the EMP formation. Finally, in Sec. V we conclude the paper.

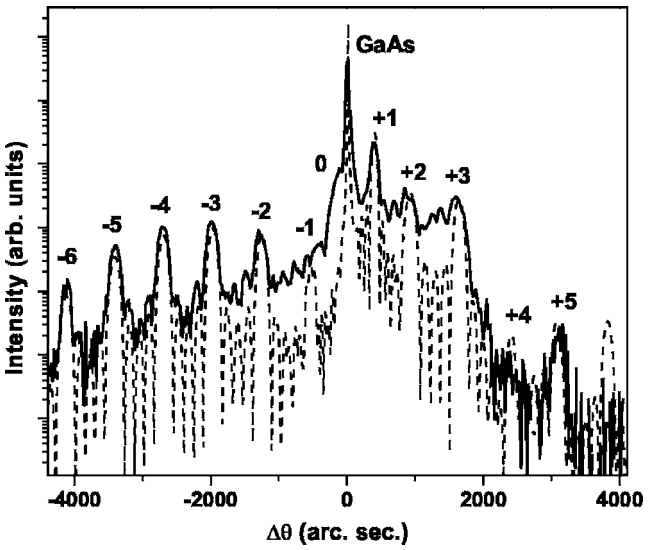

FIG. 2. $\Theta-2\Theta$ rocking curve of x-ray diffraction, measured (solid curve) and simulated (dashed curve) for the (004) reflection.

II. SAMPLE DESCRIPTION

The sample with ZnSSe/ZnMnSe multiple QW's was grown on a GaAs(001) substrate by molecular beam epitaxy in a two-chamber setup. A GaAs buffer layer was first deposited in the III-V chamber, and then the sample was transferred through the ultrahigh-vacuum module into the other chamber for II-VI growth. Ten periods of the $ZnS_{0.16}Se_{0.84}$ (19 nm)/$ZnMn_{0.16}Se_{0.84}$ (7.5 nm) structure were sandwiched between thick layers of ZnMgSSe solid alloy with the band-gap energy $E_g \sim 2.95$ eV, lattice-matched to GaAs. The thicknesses of the ZnSSe and ZnMnSe layers were chosen to meet two criteria. First of all, the balance between the tensile strain in ZnSSe and compressive strain in ZnMnSe was carefully engineered to ensure pseudomorphic growth of the structure containing layers with considerable mismatch of the lattice constant.[21] Furthermore, both ZnSSe and ZnMnSe layers were grown thick enough, in order to guarantee a reasonably long radiative lifetime of excitons in the type-II QW's. The exciton energy and radiative lifetime were calculated using the self-consistent variational method, taking into account a redistribution of carrier density due to the electron-hole Coulomb attraction.[23] The conduction- and valence-band lineups of one period of the multiple QW structure at zero magnetic field, as well as the calculated electron and heavy-hole probability distributions within the exciton, are shown in Fig. 1. All parameters of the materials were taken as in Ref. 21. For a zero magnetic field, the calculation results in a radiative lifetime of the ground excitonic state as long as 3.4 ns and a respective exciton binding energy 7.5 meV.

Figure 2 shows an x-ray diffraction $\Theta-2\Theta$ rocking curve both measured (solid curve) and simulated (dashed curve) in the sample for the (004) reflection. The rocking curve demonstrates well pronounced satellite reflections from the periodic multiple QW structure and fringes due to the interference within thick cladding layers. Both observations confirm good planarity of interfaces and low density of defects in the

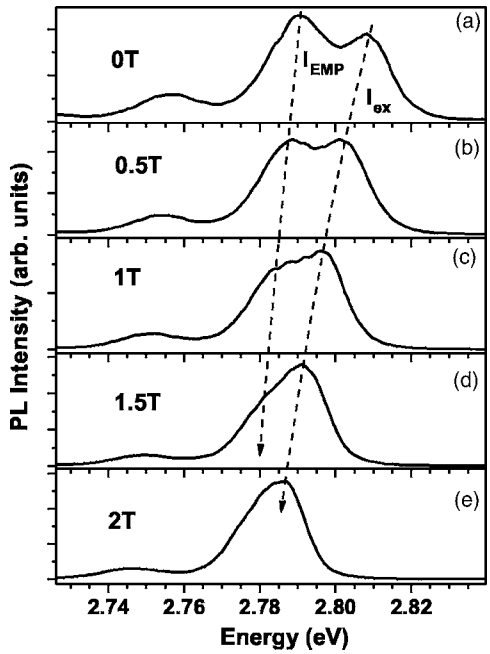

FIG. 3. Time integrated σ^+ PL spectra measured at 1.9 K with excitation power density 20 W/cm^2 at different magnetic fields. The magnetic field values are given in the figure.

sample. The position of the zero-order satellite almost exactly coincides with the reflection from GaAs, which proves the lattice matching of the multiple QW structure to the substrate as a whole.

III. OPTICAL STUDIES

A. Time-resolved PL spectra versus magnetic field and excitation power density

Time-resolved PL spectra were measured using double- or triple-frequency emission of a subpicosecond mode-locked Ti:sapphire laser. A Hamamatsu streak camera was used for the PL detection. The setup time resolution was estimated as 15–20 ps. The sample was placed in a temperature-variable Oxford He cryostat with a superconducting split-coil magnet. The Faraday geometry was used in all experiments described here. The PL in the sample was excited by linearly polarized light, whereas circular polarization of the emitted light was analyzed using a quarter-wave plate and a linear polarizer. The diameter of the excitation light spot on the sample was in the range of 0.3–0.5 mm.

One of the distinctive properties of EMP's is their suppression by the application of an external magnetic field. When the external magnetic field is much stronger than the internal effective field within the EMP, all Mn spins in the sample are equally aligned along the field direction, and the EMP binding energy is equal to zero. Figure 3 shows PL spectra time integrated over the first 2 ns after the excitation, measured at different magnetic fields. At zero magnetic field [see Fig. 3(a)] the spectrum consists of two well resolved peaks at 2.79 and 2.81 eV and their LO-phonon replica. An increase in the magnetic field results in a shift of both peaks toward lower energy. The position of the higher-energy peak reasonably follows the estimated shift of the heavy-hole band edge in the DMS ZnMnSe layer, described by a modified Brillouin function.[24] The shift of the lower-energy peak is less pronounced, so that the gap between the peaks decreases with the magnetic field increase, and at 2–3 T only one peak remains in the spectrum. It is clearly seen in Fig. 3 that the remnant peak is the higher-energy one, while the relative intensity of the lower-energy peak decreases with the magnetic field increase, and finally this peak disappears. Both peaks are strongly (nearly 100%) σ^+ polarized, even at weak magnetic fields, which is usual for DMS structures characterized by giant spin splittings and a fast rate of spin relaxation. Therefore only σ^+ polarized spectra are shown in Fig. 3.

The behavior of the higher-energy peak in the external magnetic field can be described in all details by the effect of a giant Zeeman splitting of a heavy-hole exciton in the ZnSSe/ZnMnSe type-II QW.[21] On the other hand, the performance of the lower-energy peak matches the expected behavior of the EMP. This interpretation is strongly supported by the analysis of time-resolved and temperature-dependent PL spectra, as is shown later in the paper. Therefore in the following discussion we label the two peaks as I_{ex} (higher-energy peak) and I_{EMP} (lower-energy peak).

Figure 4 shows the time-resolved PL spectra measured at different delay times after the excitation pulse at zero magnetic field for two levels of excitation: 10 W/cm^2 (Figs. 4(a)–4(d)) and 70 W/cm^2 (Figs. 4(e)–4(h)) of the average power density. Both peaks, I_{ex} and I_{EMP}, shift with the delay time toward lower energies. Furthermore, their relative intensity depends both on the delay time and excitation power density. For both levels of excitation, the increase in the delay time results in a redistribution of intensity in favor of the lower-energy I_{EMP} peak, which follows the relaxation of the energy of localized excitons and the reduction of the total density of carriers in the system due to recombination processes. On the other hand, the increase in the carrier density due to the enhanced excitation power leads to the relative enhancement of the I_{ex} peak at any delay time. Comparing the left and right columns in Fig. 4, one can notice that the spectrum measured at some delay at the high excitation level reproduces the spectrum measured at the lower excitation level but at some smaller delay time. The spectrum plotted in Fig. 4(h) (70 W/cm^2, 1125 ps) for example practically replicates the spectrum shown in Fig. 4(c) (10 W/cm^2, 215 ps). One can assume therefore that the shape of the spectrum is essentially determined by the total density of photoexcited carriers in the structure, and the two spectra correspond to nearly the same density of carriers. These observations indicate saturation of the I_{EMP} peak with an increase in the total density of photoexcited carriers. The saturation is especially remarkable at small delays after excitation, then, with an increase in delay, the saturation vanishes due to the gradual decrease in the number of the carriers in the system. The higher is the excitation density, the longer delay is needed to relax the saturation. Indeed, at the power density 10 W/cm^2 the two peaks are of comparable intensity yet at 150–200 ps after the excitation, whereas at the power density 70 W/cm^2 the I_{ex} peak dominates the spectrum up to 600–700 ps.

Similar conclusions can be deduced from the transient behavior of PL, as illustrated by the decay curves in Fig. 5.

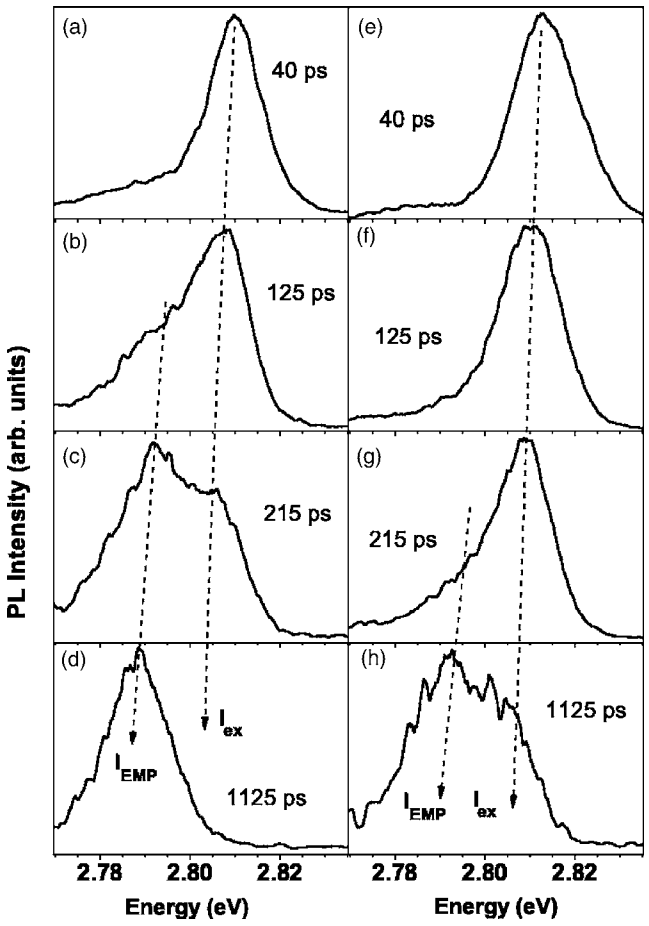

FIG. 4. Time resolved PL spectra measured at 0 T with the average excitation power density 10 W/cm^2 (a)–(d) and 70 W/cm^2 (e)–(h) at the following delay times: 40 ps (a), (e), 125 ps (b), (f), 215 ps (c), (g), and 1125 ps (d), (h).

The solid and dashed curves were detected at the wavelengths corresponding to the maxima of the I_{ex} (solid curve) and I_{EMP} (dashed curve) peaks in the time integrated spectrum at the zero magnetic field. At the relatively small level of excitation 10 W/cm^2 (see Fig. 5(a)), the two curves reflect a "two-level" behavior with the transfer of excitations from the higher-energy level (I_{ex}) to the lower-energy one (I_{EMP}). After the fast rise, the I_{ex} peak decays by nearly two orders of magnitude within 300–400 ps, while the I_{EMP} peak simultaneously gains intensity. The decay time constant for the I_{ex} peak in this range of time is about 80 ps. At the higher level of excitation 70 W/cm^2 (see Fig. 5(b)) the rise time of the I_{EMP} peak exactly matches that of the I_{ex} peak. After that the I_{EMP} peak saturates and its intensity is nearly constant within the following 500–700 ps. At longer delays, this peak decays with the time constant 3–4 ns. The estimation of this decay time is quite rough, since the period of the laser pulses is only 12 ns and the I_{EMP} peak does not decay completely within one period. The decay of the I_{ex} peak at the higher excitation power density 70 W/cm^2 is strongly nonexponential. However, even at small delay time after the excitation the decay constant exceeds 200 ps, i.e., it is two to three times longer than the respective decay time at the lower excitation power density 10 W/cm^2.

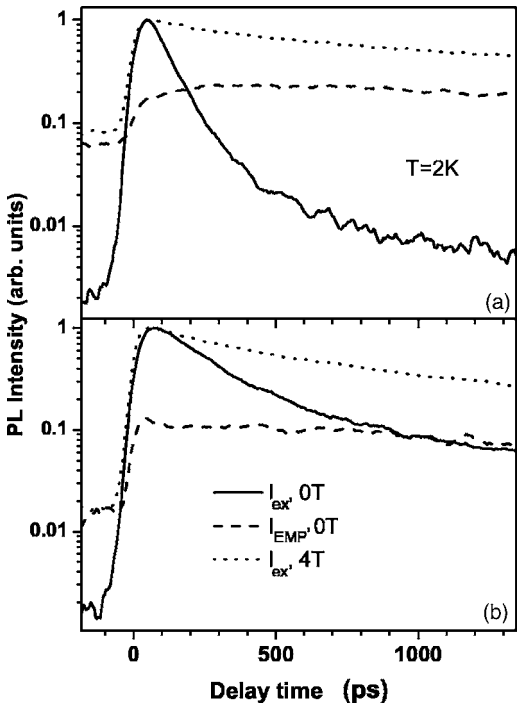

FIG. 5. PL decay curves measured at the maxima of the peaks observed in the time-integrated spectrum. The excitation power density is either 10 W/cm^2 (a) or 70 W/cm^2 (b). Solid and dashed curves correspond to the I_{ex} and I_{EMP} peaks, respectively, at a zero magnetic field. Dotted curves represent the decay of I_{ex} at 4 T. For each level of excitation, the PL intensity is normalized to the maximum of the respective I_{ex} curve.

The dotted lines in Figs. 5(a) and 5(b) represent the decay curves obtained at the magnetic field 4 T after spectral integration over the I_{ex} peak. At this relatively strong magnetic field the magnetic localization mechanisms are prohibited, and the I_{EMP} peak is completely suppressed. The decay of I_{ex} is at 4 T much slower than at the zero magnetic field. The dominant decay constant is now above 2.5 ns, in reasonable agreement with the lifetime calculation for excitons in the type-II QW. This observation suggests that the much faster decay of this peak, observed at a zero magnetic field, is due to the transfer of the excitations to the I_{EMP} level.

To directly display the interplay between the magnetic and nonmagnetic localization mechanisms, we plot in Fig. 6 the energy of the dominant peak in the PL spectrum versus the magnetic field for different delay times: immediately after excitation (filled squares), after 1.5 ns (asterisks), and after 12 ns (open circles). The excitation power density was 10 W/cm^2. As can be seen from Figs. 3 and 4 only the I_{ex} peak is visible at zero delay time for any magnetic field. In contrast to that the I_{EMP} peak is the dominant one at both 1.5 and 12 ns delay at the magnetic fields below ~2 T. At higher fields the I_{EMP} peak merges into the I_{ex} one and finally disappears. As a result, the data corresponding to 6 T illustrate the contribution to the exciton localization from nonmagnetic mechanisms. Assuming the exciton to be practically free at zero delay time, one can deduce that most of the localization occurs within the first 1.5 ns, and at 12 ns the system is close to quasiequilibrium. Then the nonmagnetic part of the exci-

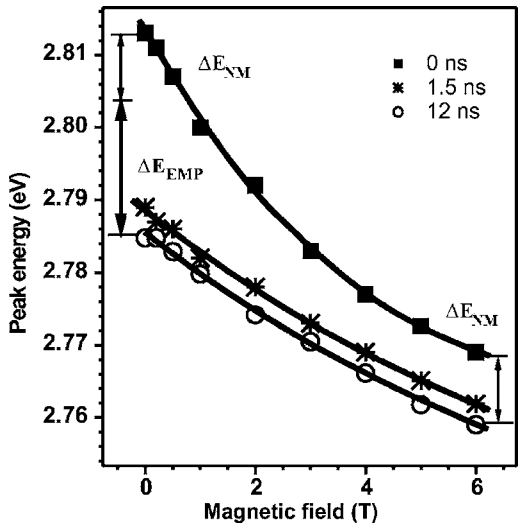

FIG. 6. PL peak energy versus magnetic field, measured at 2 K with the excitation power density 10 W/cm^2 at different delay times: 0 ns (solid squares), 1.5 ns (asterisks), and 12 ns (open circles). Solid curves are drawn only to guide the eye.

ton localization energy ΔE_{NM} can be estimated as 7–8 meV, as demonstrated in Fig. 6. Bearing in mind that the localization mechanisms of nonmagnetic origin only weakly depend on the magnetic field, the binding energy of the EMP at zero magnetic field ΔE_{EMP} can be estimated as 18–20 meV.

B. Temperature-dependent time-resolved PL

To elucidate peculiarities of the exciton localization process we have measured time-resolved PL spectra at different temperatures. The increase in temperature decreases the EMP binding energy and finally suppresses the EMP formation. Therefore the experiments at variable temperature allow one to control the relative contributions from magnetic and nonmagnetic mechanisms of the exciton localization. In particular, the I_{EMP} peak in the studied sample is completely suppressed at 20 K. Figure 7 demonstrates how the energy (a) and integral intensity (b) of the I_{ex} (open circles) and I_{EMP} (solid squares) peaks depend on the temperature at zero magnetic field. These characteristics were measured at the 1.5 ns delay time, since at this long delay the two peaks can be readily separated by decomposition of the spectrum into two Gaussian peaks. With the temperature increase the I_{EMP} energy increases, which is an expected behavior for the EMP. Simultaneously, the I_{ex} peak shifts toward lower energies. This shift can hardly be attributed to the effect of the temperature-induced bandgap shrinkage, since the respective shift should be negligibly small at these temperatures. Anyway, the absence of the shift toward higher energies clearly indicates the negligible impact of magnetic localization on the excitonic states responsible for the I_{ex} peak. The temperature dependences of the integral intensity (see Fig. 7(b)) for the two peaks are also opposite. The temperature increase quenches the I_{EMP} peak, but enhances the I_{ex} one. As a result, the total PL intensity of the sample only weakly depends on the temperature in this range. The increase in temperature

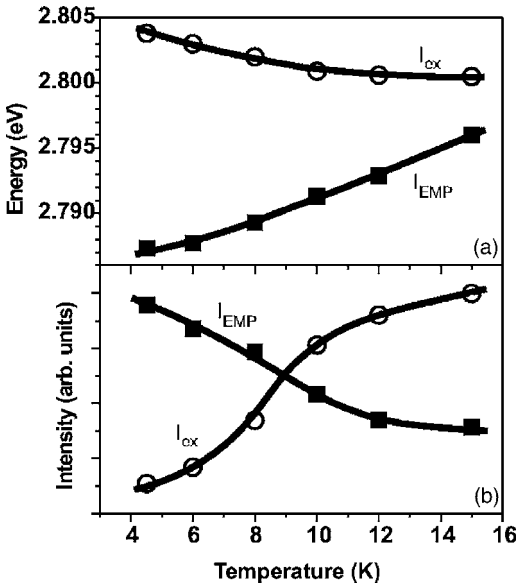

FIG. 7. I_{ex} (open circles) and I_{EMP} (solid squares) peak energies (a) and integral intensities (b) versus temperature at the zero magnetic field and 1.5 ns delay time. Solid lines are plotted to guide the eye. The excitation power was 20 W/cm^2.

rather results in the redistribution of the intensities of the two peaks due to suppression of the EMP formation process.

Figure 8 shows two series of time-resolved spectra measured at 4.5 K (solid curves) and 20 K (dashed curves) at relatively small delay times. It is seen in Fig. 8(a) (delay time 22 ps) that immediately after excitation the I_{ex} peak energy is practically the same for both temperatures. The shape of the spectrum at small delays is quite complicated. However, yet at the 135 ps delay time (Fig. 8(c)) the I_{ex} peak energy is

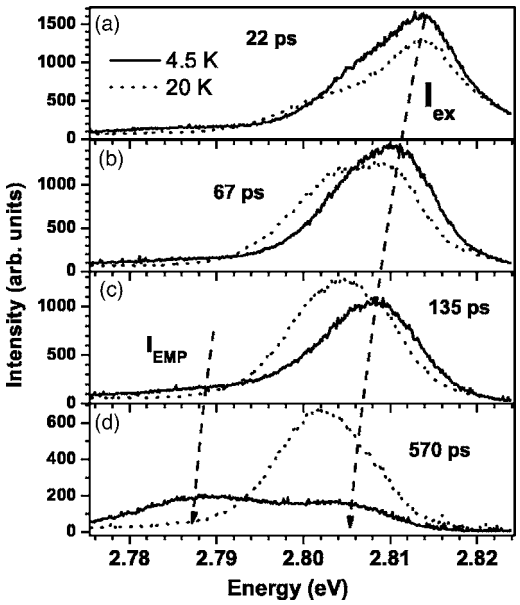

FIG. 8. Time-resolved PL spectra measured at 4.5 K (solid curves) and 20 K (dotted curves) at different delay times pointed in the figure. The excitation power density was 20 W/cm^2 and the magnetic field was zero.

obviously different for the two temperatures. At longer delays the spectrum at 20 K consists of a single I_{ex} peak, while the spectrum at 4.5 K comprises both the I_{ex} and I_{EMP} peaks (see Fig. 8(d)). This complicated behavior observed in the region of small delays suggests that the "red" shift of the I_{ex} peak displayed in Fig. 7(a) results from the temperature-dependent localization process rather than the temperature-induced variation of the bandgap energy.[25]

To summarize the results of the optical experiments, the main findings described in this section can be formulated as follows:

(i) Both the I_{ex} and I_{EMP} peaks are due to the emission of type-II localized excitons in the ZnSSe/ZnMnSe QW. The radiative lifetime of these excitons exceeds ~3 ns.

(ii) The dominant exciton localization mechanism for the I_{ex} peak is of a nonmagnetic origin, whereas the appearance of the I_{EMP} peak is attributed to the formation of EMP with a binding energy 18–20 meV;

(iii) At relatively small excitation power density (~10 W/cm^2 and less) the I_{ex} peak rapidly decays with the characteristic time constant ~80 ps due to energy relaxation of the involved excitons. This relaxation process is presumably of magnetic origin, since it results in the enhancement of the I_{EMP} peak. At higher levels of excitation this relaxation channel is suppressed, and the intensity of the I_{EMP} peak is saturated.

IV. DISCUSSION

In this section we focus on the discussion of density-dependent effects in the time-resolved PL spectra. All the measurements reported here were performed in the intermediate regime, when the density of photoexcited electron-hole (e-h) pairs is below the exciton Mott density. The latter can be estimated as more than 1×10^{12} cm^{-2} per one QW, whereas the maximum averaged excitation power density used (70 W/cm^2) results in no more than 1.7×10^{11} cm^{-2} sheet density of injected e-h pairs per one pulse per one QW. Under these conditions the many-body interactions are not important and the density-dependent effects should be restricted to band bending induced by charge separation in the type-II QW, light-induced heating effects, and specific spin-related effects relevant to the EMP formation.

The electrostatic bending of the QW potential occurs in type-II QW's due to the spatial separation of photoexcited electrons and holes. It usually results in a higher-energy shift of the excitonic emission line and a reduction of the exciton radiative lifetime.[26] Both effects can be deduced from the analysis of time-resolved spectra and decay curves, shown in Figs. 4 and 5. In particular, comparing the behavior of the dotted curves in Figs. 5(a) and 5(b), one can conclude that an increase in the excitation power density somewhat accelerates the PL decay. Since these curves were measured at 4 T, when the I_{EMP} peak is completely suppressed, this observation directly indicates the density-induced increase in the recombination rate of excitons. Furthermore, both the I_{ex} and I_{EMP} peaks slightly shift to higher energies with increasing power density at a fixed delay time. The maximum density-induced shift of the PL peaks, observed in the used range of excitation power densities at any particular delay time, does not exceed ~5 meV. This is four times smaller than the estimated binding energy of the EMP at 0 T. Accordingly, the relaxation and recombination dynamics of the EMP's is determined at the zero magnetic field by the magnetic localization rather than by the band-bending effects. On the other hand, the shift of the I_{ex} peak, induced by the carrier-induced electrostatic effects, can be comparable with the nonmagnetic part of the exciton localization energy. Therefore the nonmagnetic localization energy determined in Sec. III A as 7–8 meV can be overestimated.

The discussed experiments were carried out at relatively high excitation levels. Therefore the effects of optical heating of the magnetic ion system can be quite pronounced. Previously these effects were studied in DMS structures with a relatively small content of Mn (less than 7%).[27,28] Two heating mechanisms were proposed. One mechanism is the total heating of the structure due to the light absorption in the GaAs substrate.[28] This process is rather slow and should be completely integrated on the nanosecond time scale of interest. The other mechanism implies the direct transfer of energy from photoexcited carriers into the magnetic ion system due to spin-flip exchange scattering.[27] The cooling of the Mn system in this case relies on the process of spin-lattice relaxation, which is quite slow in DMS. For example, for a ZnMnSe QW with 6% of Mn the spin-lattice relaxation time is as long as about 160 μs.[27] The spin-lattice relaxation rate drastically increases with a growing concentration of Mn ions, which leads to suppression of the heating efficiency. We have not found in the literature any data on the spin-lattice relaxation rate in DMS structures with the Mn content as high as in our sample (16%). However, extrapolation of the data collected by Dietl *et al.* (Ref. 29) allows one to estimate the respective value as not exceeding 10^8 s^{-1}. It means that the heating and cooling of the Mn ions due to the second mechanism also does not influence the subnanosecond dynamics of EMP's, but rather results in a certain average overheating of the magnetic ion system. One should note that the EMP itself can be used to estimate the heating efficiency. As was shown in Sec. III B, the increase in the temperature causes drastic quenching and a blue shift of the I_{EMP} peak (see Fig. 7). None of these effects is remarkable in the studied range of excitation power densities (compare, e.g., left and right columns in Fig. 4). Therefore we conclude that the efficiency of optical heating is quite weak in the studied sample with a high concentration of Mn ions, and, as a first approximation, the influence of the light-induced heating can be neglected.

The most remarkable density-dependent effect observed in our experiments is the redistribution of the I_{ex} and I_{EMP} intensities, up to the complete saturation of the I_{EMP} peak at quite moderate excitation power densities. One can assume that the explanation of this effect should rely on some dynamical aspects of the EMP formation. It is accepted at present that the EMP formation is controlled by two processes.[29,30] First, a certain time is needed to align the spins of the Mn^{2+} ions. Usually this process can be characterized by a single time-constant τ_s with a value limited by the spin-spin relaxation rate. Second, the exciton wave function changes during the EMP formation and, hence, the EMP

formation time τ_f can be much longer than τ_s. A simple analytical model describing the dynamics of the EMP formation was developed by Yakovlev and Kavokin (see Ref. 30). According to this theory, the evolution of the EMP energy in time follows an exponential law of relaxation:

$$E(t) = E_f(1 - e^{-t/\tau_f}), \tag{1}$$

where the formation time is given by

$$\tau_f = \tau_s \cdot \frac{E_f}{E_0}, \tag{2}$$

E_f is the EMP equilibrium energy at its final state (at infinite time), and E_0 is the equilibrium energy at the initial state ($t=0$), as determined by the conditions of initial localization. The equilibrium energy values correspond to the exchange field $B_{ex}(\mathbf{r},t)$ created by the exciton. The exchange constant for holes in ZnMnSe is five times larger than for electrons, and usually the hole contribution dominates the EMP formation. In the studied sample the electron contribution can be neglected completely due to the small overlap of the electron wave function with the diluted magnetic part of the type-II QW structure. As a result, the carrier-induced exchange field is proportional to the squared modulus of the hole wave function and, hence, inversely proportional to the localization volume of the hole. At each time the equilibrium energy (E_{eq}) and the hole localization volume (V) can be linked, using the following expression (see Ref. 14):

$$E_{eq} = N_0^{-1} x S_{eff} \frac{s+1}{12} \frac{(N_0\beta)^2}{k_B(T+T_0)} \frac{1}{V}, \tag{3}$$

where N_0 is the number of cation sites in the unit volume, x is the Mn mole fraction in $Zn_{1-x}Mn_xSe$, $s=5/2$ is the spin of a Mn ion, β is the constant of the exchange interaction for the valence band, and k_B is the Boltzmann constant. The effective spin S_{eff} and T_0 are phenomenological parameters. Their values for ZnMnSe are well known (see, e.g., Ref. 21 and references therein).

Equations (1)–(3) allow one to link the experimentally measured EMP binding energy at the final state (E_f) and the EMP formation time (τ_f) with the hole localization volume, both at the initial and final states of the EMP. We have not found in the literature any systematic data on the experimental measurements of the spin-spin relaxation rate in ZnMnSe solid alloys. However, as a rough estimation, one can take the τ_s value known for $Cd_{1-x}Mn_xTe$ alloys, since the properties of the Mn subsystem in II-VI DMS do not depend significantly on the properties of the matrix. For $x=0.16$, the τ_s value should be in the range of 50–100 ps.[29]

In principle, the experimental value of τ_f can be extracted from the fit of the EMP emission energy versus the delay time. However, at the initial delay times (less than 100–150 ps) the I_{EMP} peak emerges as a weak shoulder of the more intensive I_{ex} peak. Therefore it is impossible to extract the EMP emission energy from the experimental data with reasonable accuracy. One can notice nevertheless that just being formed the I_{EMP} peak practically does not shift with the delay time. This allows one to estimate τ_f at the zero magnetic field as less than ~100 ps. Another way to estimate τ_f is to measure the decay time of the I_{ex} peak at a low excitation power density, since at these conditions the dominant mechanism of the I_{ex} decay is the EMP formation. The measured ~80 ps value for the dominant decay time of the I_{ex} peak (see the solid curve in Fig. 5(a)) specificates the upper limit for the EMP formation time τ_f. This value is very close to the estimated spin-spin scattering rate τ_s. It follows then from Eq. (2) that $E_f \approx E_0$ and, hence, the variation of the exciton wave function during the EMP formation is negligibly small. Using the value of EMP binding energy 20 meV, we obtain from Eq. (3) the hole localization volume 320 nm^3. For the 7.5 nm thick ZnMnSe QW, this value corresponds to the two dimensional (2D) hole localization radius ~3.7 nm. One should emphasize that this size is determined by some mechanism of hole localization other than the exchange interaction with Mn ions, and the EMP formation does not result in any remarkable additional shrinkage of the hole wave function.

The previous consideration concerned the excitons emitting within the I_{EMP} peak, with the relatively large EMP binding energy (~20 meV) and fast EMP formation time (<80 ps). There is another type of localized exciton in the structure, emitting within the I_{ex} peak. The EMP formation time for these excitons should be quite long, since the process of magnetic localization is practically unobservable within the I_{ex} peak lifetime that at relatively strong excitation approaches 1–2 ns (see the solid curve in Fig. 5(b)). According to Eq. (2), a long EMP formation time implies $E_f \gg E_0$. It means that the hole localization volume at the initial EMP state should be much larger than at the final EMP state. For example, if we assume that $\tau_f=2$ ns and the hole localization volume in the final EMP state is 320 nm^3, which corresponds to the 20 meV EMP binding energy, then the hole localization volume in the initial EMP state can be obtained from Eqs. (2) and (3) as 9140 nm^3. This value corresponds to the 2D hole localization radius 19.7 nm. This estimation shows that for a quite realistic hole localization radius ~20–30 nm at the initial EMP state, the EMP formation process can be practically unobservable, even on the nanosecond time scale.

According to this estimation, the coexistence of the two emission peaks can be explained by the occurrence of hole localization sites with different localization radii. The holes trapped in the sites with the small localization radius (~4 nm) rapidly decrease their energy by about 20 meV due to the EMP formation. The recombination of the respective excitons contributes to the I_{EMP} emission peak. Other holes, trapped in the sites with the large localization radius (20–30 nm), cannot form EMP's within the practical time. At relatively low excitation power densities, the PL lifetime within the I_{ex} peak is limited by carrier tunneling between localized states toward the sites suitable for the EMP formation. When the hole encounters such a site with the small localization radius, it forms the EMP on the time scale comparable with the spin-spin scattering time τ_s. In the transient PL spectra it appears like the redistribution of the relative intensity between the I_{ex} and I_{EMP} peaks with a delay time. On the other hand, when the density of the photoexcited e-h pairs is comparable with the density of the hole localization sites with small radii, most of these sites are filled, which suppresses the formation of EMP's and results in the satura-

tion of the I_{EMP} peak intensity. This saturation effect is noticeable at small delays after the excitation at the power densities higher than ~ 10 W/cm^2. The respective peak sheet density of photoexcited holes per one QW can be estimated as $\sim 2 \times 10^{10}$ cm^{-2}. This value can be considered as a rough evaluation of the density of the localization sites with small radii.

The proposed explanation of the observed density-dependent effects implies a specific structure of the hole localization potential. Indeed, according to Eqs. (1)–(3) a simple Gaussian-like probability distribution of the localization sizes would result in a single-peak smooth distribution of the EMP energies $E(t)$ at any particular time t. This contradicts the experimental observation of two emission lines practically at any delay time after the excitation. Therefore, one can rather expect the bimodal distribution of the size of the hole localization sites with one peak at small sizes (~ 4 nm) and the other peak at large sizes (>20 nm). The emergence of at least two different localization mechanisms follows also from the complicated shape of the excitonic emission spectrum measured at 20 K at initial delay times (see the dotted curves in Fig. 8).

Our experiments provide no data about the microscopic nature of the localization potential. Nevertheless, it seems useful to discuss briefly the main peculiarities of localization mechanisms in the studied structure. The most intriguing feature is an expected weak contribution of the majority of the localization processes observed usually in semiconductor QW's. Since the studied QW's are relatively wide, the contribution from the well thickness fluctuations should be negligibly small. Furthermore, the influence of the alloy disordering effects should also be reduced due to the specific properties of the ZnSSe and ZnMnSe solid alloys and the type-II band lineup of the structure. In the ternary compound ZnSSe, the variation of the S content affects only the position of the valence band edge, leaving the conduction band edge energy practically unchanged.[31] Therefore the fluctuations of the S content practically do not contribute to the fluctuating potential sensed by electrons confined in the ZnSSe QW. In contrast to that, the variation of the Mn content in the ZnMnSe ternary solid alloy affects mainly the energy of the conduction band edge[32,33] and, hence, the fluctuations of the alloy composition only weakly affect the localization of holes confined in the ZnMnSe QW.

On the other hand, it is well known that the intentionally undoped ZnSe-based layers contain a noticeable concentration (up to 10^{16} cm^{-3}) of intrinsic donor impurities. One can expect that most of the donors located within the relatively thin ZnMnSe conduction-band barriers will by ionized, whereas neutral donors should be dominant at low temperatures in the ZnSSe electron wells. These two types of donors can differently contribute to the hole localization—either as a result of the fluctuating potential induced by the ionized donors in ZnMnSe or due to the formation of type-II D^0X complexes, involving two electrons confined in the ZnSSe and one hole confined in ZnMnSe. In both cases the hole localization radius should be quite extended. For the field of ionized donors, which are Coulomb repulsive centers for the holes, the characteristic size of the potential fluctuations should be of the order of the average distance between the donors. For the donor concentration 10^{16} cm^{-3} it can be estimated as ~ 46 nm. The radius of the hole orbit within the type-II exciton bound to a neutral donor drastically depends on the exact position of the donor with respect to the ZnSSe/ZnMnSe heterojunction. In any case, it should be a few times larger than the radius of the hole orbit, estimated for a bulk D^0X complex in ZnSe as ~ 7 nm.[34] On the basis of this analysis we tentatively suggest that the sites with a large localization volume result from the Coulomb interaction of the hole with either ionized or neutral donors. The most probable origin of the sites with a small localization volume is due to fluctuations of the ZnMnSe alloy composition, associated presumably with the effect of Mn clustering.[35]

Finally, we briefly comment on the peculiarities of exciton dynamics in the type-II DMS QW's with the relatively small exciton binding energy. It seems possible that the energy relaxation of photoexcited carriers in such structures is dominated by separate relaxation of electrons and holes rather than relaxation of the exciton as an entity. After fast cooling down the bottoms of the respective bands, the carriers couple into the excitons and suffer from additional localization due to either magnetic or nonmagnetic mechanisms. Since the energy of the magnetic localization of the hole is at least three times larger than the exciton binding energy, the Coulomb interaction between the electron and hole only weakly influences the process of magnetic localization. This circumstance validates the neglect of the Coulomb interaction between the electron and hole in the performed analysis of the EMP formation process. On the other hand, the shrinkage of the excitonic wave function due to the magnetic localization of the hole affects the recombination dynamics of the EMP. This results in the enhanced radiative lifetime of the EMP as compared with the lifetime of weakly localized excitons contributing to the I_{ex} emission line. The latter excitons are presumably localized due to interaction with donors and, hence, the Coulomb interaction between the electron, the hole, and the impurity center cannot be ignored in any accurate description of this nonmagnetic localization process.

V. CONCLUSIONS

Summarizing, we have studied density-dependent dynamics of exciton localization in ZnSSe/ZnMnSe type-II QWs in the range of moderate densities well below the exciton Mott density. At low excitations below ~ 10 W/cm^2 the spectra demonstrate the efficient formation of EMP's, while the increase in the power density results in fast saturation of the EMP formation and the accumulation of a large density of long-living excitons localized due to some nonmagnetic mechanism. This behavior implies a rather limited density of the exciton localization sites with the localization radius small enough to ensure the fast formation of EMP's with noticeable binding energy. The observed density-dependent behavior differs from the previously considered scenarios, suggesting that the increase in the excitation power density either gradually destroys EMP's,[20] or results in the formation of a "collective exciton magnetic polaron."[18] To explain the observed easy saturation of the EMP recombination, one should assume that the formation of magnetic bipolarons

(and multipolarons) in the studied QW's is a rather unlikely process. Otherwise, the EMP's formed in the most suitable sites with a small localization radii would serve as nucleation centers, leading to the fast condensation of the rest of the excitons within ferromagnetic domains. In contrast to that, the number of EMP's in the studied structure is strongly limited by the number of the suitable localization sites. The excess of photoexcited e-h pairs leads to the formation of weakly localized excitons characterized by large localization radius and very long EMP formation time.

ACKNOWLEDGMENTS

This work was supported by the Program of the PS department of RAS and RFBR. A. A. T. acknowledges support from the Wenner-Gren Foundation, Sweden, and from the Russian Science Support Foundation. Support by the Ministry of Education, Science, and Culture, Japan, and by NEDO Nanotechnology Materials Program, Japan, are also acknowledged.

[1] P. A. Wolf, in *Semiconductors and Semimetals*, edited by J. K. Furdyna and J. Kossut (Academic, London, 1988), Vol. 25, p. 413.
[2] J. H. Harris and A. V. Nurmikko, Phys. Rev. Lett. **51**, 1472 (1983).
[3] A. Golnic, J. Ginter, and J. A. Gai, J. Phys. C **16**, 6073 (1983).
[4] Y. Oka, K. Nakamura, I. Souma, M. Kido, and H. Fujisaki, J. Lumin. **38**, 263 (1987).
[5] G. Mackh, W. Ossau, D. R. Yakovlev, A. Waag, G. Landwehr, R. Hellmann, and E. O. Göbel, Phys. Rev. B **49**, 10248 (1994).
[6] M. Nogaku, J. X. Shen, R. Pittini, T. Sato, and Y. Oka, Phys. Rev. B **63**, 153314 (2001).
[7] D. R. Yakovlev, W. Ossau, G. Landwehr, R. N. Bicknell-Tassius, A. Waag, and I. N. Uraltsev, Solid State Commun. **76**, 325 (1990).
[8] D. R. Yakovlev, G. Mackh, B. Kuhn-Heinrich, W. Ossau, A. Waag, G. Landwehr, R. Hellmann, and E. O. Göbel, Phys. Rev. B **52**, 12033 (1995).
[9] T. Stirner, J. Miao, W. E. Hagston, S. Takeyama, G. Karczewski, T. Wojtowicz, and J. Kossut, Phys. Rev. B **60**, 11545 (1999).
[10] C. D. Poweleit, L. M. Smith, and B. T. Jonker, Phys. Rev. B **50**, 18662 (1994).
[11] V. V. Rossin, F. Henneberger, and J. Puls, Phys. Rev. B **53**, 16444 (1996).
[12] C. Benoit à la Guillaume, Yu. G. Semenov, and M. Combescot, Phys. Rev. B **51**, 14124 (1995).
[13] G. Mackh, M. Hilpert, D. R. Yakovlev, W. Ossau, H. Heinke, T. Litz, F. Fischer, A. Waag, G. Landwehr, R. Hellmann, and E. O. Göbel, Phys. Rev. B **50**, 14069 (1994).
[14] K. V. Kavokin, I. A. Merkulov, D. R. Yakovlev, W. Ossau, and G. Landwehr, Phys. Rev. B **60**, 16499 (1999).
[15] T. Dietl and J. Spalek, Phys. Rev. Lett. **48**, 355 (1982).
[16] T. Stirner, W. E. Hagston, S. Takeyama, G. Karczewski, T. Wojtowicz, and J. Kossut, Physica E (Amsterdam) **10**, 331 (2001).
[17] S. V. Goupalov and A. V. Kavokin, Solid State Commun. **97**, 77 (1996).
[18] A. Kavokin, B. Gil, and P. Bigenwald, Phys. Rev. B **57**, R4261 (1998).
[19] T.-B. Sun, G. A. Balchin, L. M. Smith, and B. T. Jonker, Phys. Status Solidi A **164**, 547 (1997).
[20] T. Kuroda, A. Tatsugawa, F. Minami, S. Seto, S. Kuroda, and K. Takita, Physica E (Amsterdam) **10**, 344 (2001).
[21] A. A. Toropov, A. V. Lebedev, S. V. Sorokin, D. D. Solnyshkov, S. V. Ivanov, P. S. Kop'ev, I. A. Buyanova, W. M. Chen, and B. Monemar, Semiconductors **36**, 1288 (2002).
[22] A. A. Toropov, Ya. V. Terent'ev, A. V. Lebedev, S. V. Sorokin, V. A. Kaygorodov, S. V. Ivanov, P. S. Kop'ev, I. A. Buyanova, J. P. Bergman, B. Monemar, and W. M. Chen, Phys. Status Solidi C **1**, 847 (2004).
[23] E. L. Ivchenko, A. V. Kavokin, V. P. Kochereshko, G. R. Posina, I. N. Uraltsev, D. R. Yakovlev, R. N. Bicknell-Tassius, A. Waag, and G. Landwehr, Phys. Rev. B **46**, 7713 (1992).
[24] J. A. Gaj, R. Planel, and G. Fishman, Solid State Commun. **29**, 435 (1979).
[25] S. A. Tarasenko, A. A. Kiselev, E. L. Ivchenko, A. Dinger, M. Baldauf, C. Klingshirn, H. Kalt, S. D. Baranovckii, R. Eichmann, and P. Thomas, Semicond. Sci. Technol. **16**, 486 (2001).
[26] H. Priller, M. Schmidt, M. Dremel, M. Grün, A. Toropov, E. L. Ivchenko, H. Kalt, and C. Klingshirn, Phys. Status Solidi C **1**, 747 (2004).
[27] D. Keller, D. R. Yakovlev, B. König, W. Ossau, Th. Gruber, A. Waag, L. W. Molenkamp, and A. V. Scherbakov, Phys. Rev. B **65**, 035313 (2002).
[28] A. V. Koudinov, Yu. G. Kusrayev, and I. G. Aksyanov, Phys. Rev. B **68**, 085315 (2003).
[29] T. Dietl, P. Peyla, W. Grieshaber, and Y. Merle d'Aubigne, Phys. Rev. Lett. **74**, 474 (1995).
[30] D. R. Yakovlev and K. V. Kavokin, Comments Condens. Matter Phys. **18**, 51 (1996).
[31] C. G. Van de Walle, Phys. Rev. B **39**, 1871 (1989).
[32] E. Deleporte, T. Lebihen, B. Ohnesorge, Ph. Roussignol, C. Delalande, S. Guha, and H. Munekata, Phys. Rev. B **50**, 4514 (1994).
[33] P. J. Klar, D. Wolverson, J. J. Davies, W. Heimbrodt, and M. Happ, Phys. Rev. B **57**, 7103 (1998).
[34] M. Suffczynski and L. Wolniewicz, Phys. Rev. B **40**, 6250 (1989).
[35] S. J. Weston, M. O'Neill, J. E. Nicholls, J. Miao, W. E. Hagston, and T. Stirner, Phys. Rev. B **58**, 7040 (1998).